Single period learning for radial tracking of a CD player

Single Period Learning for radial tracking of a CD player

R.H.A. Kuypers
s445213
Traineeship report DCT 2001.62

Eindhoven, 29 November 2001

Supervised by:
Prof. Dr. Ir. M. Steinbuch

Summary

To read the information of a disk properly with a CD player, the radial error has to be less that 0.1 μm. This is achieved with an internal and a designed external PID-controller. But to make the CD-player able to resist shocks and work at higher rotational speeds in the future, a smaller radial error has to be obtained. With Single Period Learning (SPL) the fact is used that the radial error is a periodic signal. The main idea of SPL is to take 1 period of the radial error, put it into a memory loop and finally add the output signal from the memory loop, as a sort of feedforward signal, to the radial error (without any phase delay). The result is that the radial error reduces to 0.22 nm. When a phase delay occurs, the output signal is not added to the radial error at exactly the beginning of a period but a little bit earlier or later. When the phase delay lies between -14.4° ($=345.6^{0}$) and 13.3^{0} (360^{0} = exact 1 period delay) the error reduction will be at least 50%. The smaller the phase delay is that occurs the bigger the radial error reduction will be. SPL will amplify noise with a factor $\sqrt{2}$. SPL is also very sensitive for not knowing the rotational frequency. The radial error will be even larger than without using SPL. This is disappointing. At some points (overlap points) the radial error is as small as the case when the rotation frequency is exactly known. The closer the supposed frequency is to the rotational frequency the longer it takes for these overlap points to occur, but the maximum radial error stays the same. An attempt to make SPL robust with a technique, known from repetitive control, failed. The error is in that case also bigger than when SPL is not used.

Table of contents

1 Introduction

The CD-player used in this report is a carloader with a radial rotating arm (type CDm9). A picture of the radial rotating arm mechanism is shown in figure 1.1.

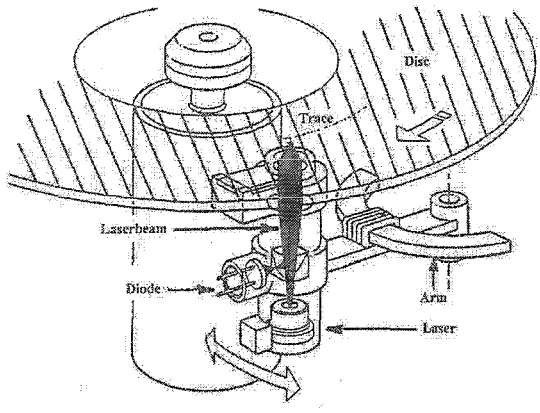

Figure 1.1: Radial rotating arm mechanism

To read the information of the disk properly, there are two actuators used to follow the track on a disk. One actuator is used to follow the track in the radial direction and one is used to focus the laserbeam on the track. So also two error signals occur: the radial error and the focus error. In this report only the radial error is of interest. To assure that the information on the disk will be read properly, the radial error has to be less than 0.1 μm. To make the CD-player able to resist shocks and work at higher rotational speeds in the future, a smaller radial error has to be obtained. So the main goal in this report is to keep this radial error as small as possible but maximal 0.1 μm.

The tracks on a perfect disk follow an exact spiral (see figure 1.2). The distance between the tracks is 1.6 μm and the tracks are 0.4 μm wide. In practice the disks are not perfect but manufactured with a maximum track eccentricity of 100 μm. The maximum radial error that is allowed is 0.1 μm. This means that the gain of the sensitivity at the rotational frequency should be less then 0.001, which is similar to –60 dB.

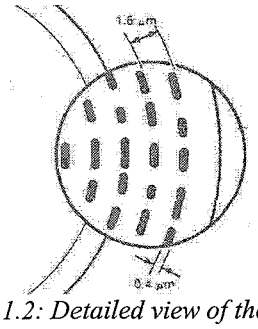

Figure 1.2: Detailed view of the disk

In chapter 2 a model for the CD player (the plant) will be derived and also an external PID-controller will be designed. In chapter 3 simulations and experiments with the internal controller and the designed external controller will be presented. In chapter 4 a method to reduce the radial error further will be discussed: Single Period Learning.
Finally conclusions and recommendations will be made in chapter 5.

2 Experimental modelling and external controller design

2.1 Experimental modelling

Before there can be done any simulations, a model of the CD player has to be optained. The model of the CD player or the plant (P) can be determined out of the following expression when the sensitivity (S) and the controller (C) are known:

$$S = \frac{1}{1+CP} \rightarrow P = \frac{S^{-1}-1}{C} \tag{1}$$

In the figure below, the measurement setup is shown.

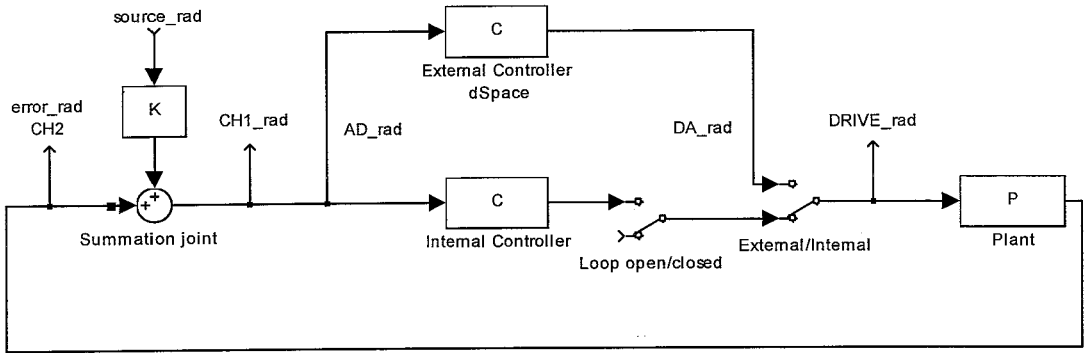

Figure 2.1: Measurement setup

The signals are measured with the Virtual Swept Sine (VSS) option in the SigLab menu. The frequency range can be split into different ranges with different accuracy levels (settings are shown in appendix A). Every frequency response is measured at exact the same frequencies, because for all the measurements the same settings are used. This makes it easier to calculated with the optained vectors.

2.1.1 Summation joint

To make sure whether the summation joint is an ideal one or not, the frequency response from source_rad to CH1 is measured. During this measurement the loop has to be opened, which can be achieved by turning off the laser. The frequency response of the summation joint is shown in figure 2.2.

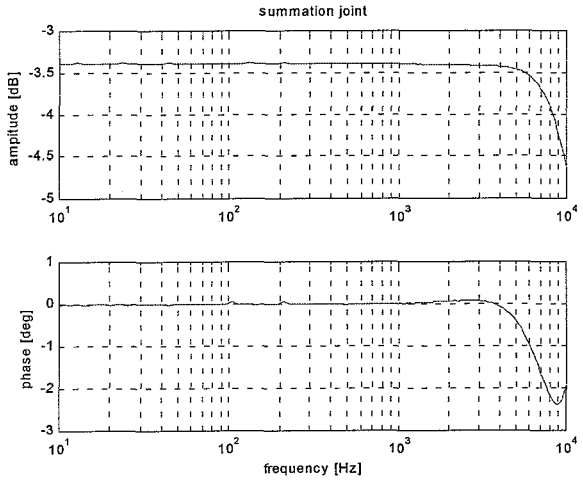

Figure 2.2: Frequency response of the summation joint

The summation joint is not an ideal one because it has a gain of -3.4 dB. Therefore the measurements of the sensitivity and the controller have to be corrected. Dividing these measurements by the frequency response of the summation joint will correct the data.

2.1.2 Sensitivity

The sensitivity can be optained by measuring the frequency response from source_rad to CH1 with the loop closed. The sensitivity, corrected for the summation joint, is shown in figure 2.3.

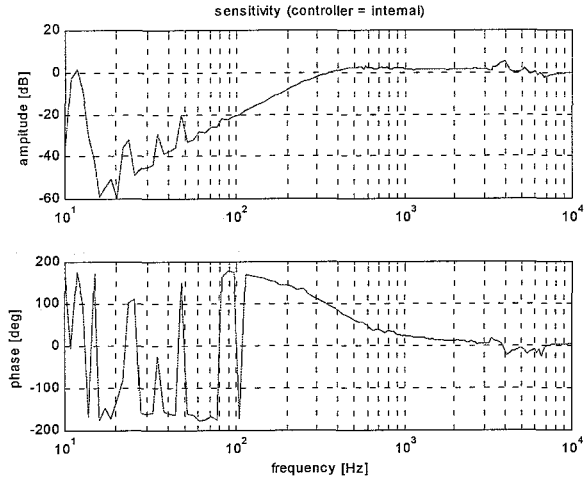

Figure 2.3: Sensitivity (with internal controller)

Peaks appear at the rotational frequency of 12 Hz and its harmonics. The coherence of the sensitivity is shown in figure 2.4. These peaks appear at the lower frequencies because the eccentricity of the disk at that point has a larger influence on the error then the noise injected in source_rad. The coherence is low between 0 and 130 Hz, so the peaks should be ignored during the fitting of the model.

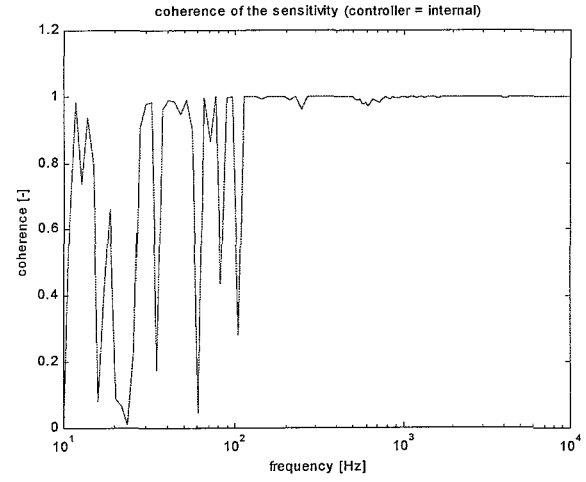

Figure 2.4: Coherence of the sensitivity (with internal controller)

2.1.3 Internal controller

The internal controller can be optained in two ways:
- by measuring the frequency response from source_rad to DRIVE_rad with the loop opened and correcting it for the summation joint.
- by using the electric charts for the print board [1]

The frequency response of the internal controller, optained by measurement as well as by using the electric charts, is shown in figure 2.5.

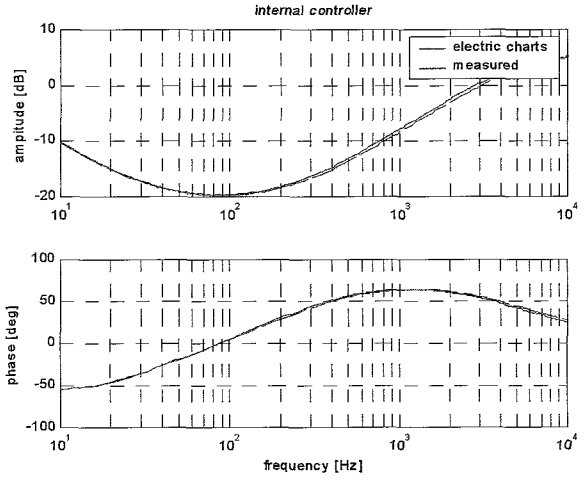

Figure 2.5: Frequency response of the internal controller

2.1.4 Plant

By using equation (1) the frequency response of the plant can be derived. This response has been fitted with a 6th order fit. Both the frequency response of the plant and its fit are shown in figure 2.6.

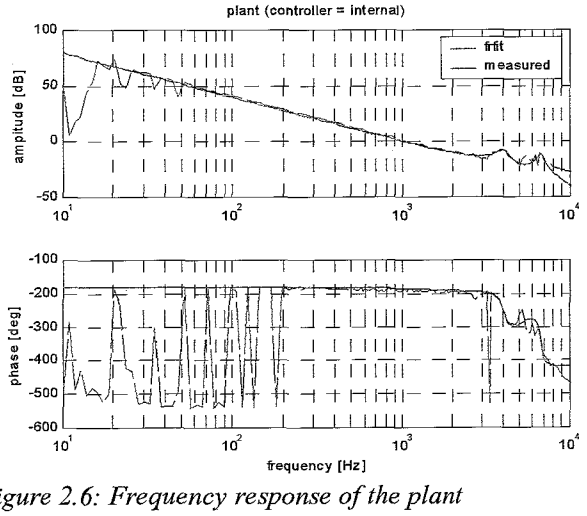

Figure 2.6: Frequency response of the plant

2.2 External PID-controller (phase 1)

An external PID-controller was designed to reduce the radial error. Specifications for this design are:
- bandwidth of 700 Hz
- the sensitivity at the rotational frequency should be less then –60 dB (see chapter 1)
- there has to be an amplitude margin of at least 2 so the maximum sensitivity should be less the 6 dB
- the phase margin has to be large enough (+/- 40°)

The characteristics of the external PID-controller, designed with DIET are:
- gain (P-action): 2.6
- zero D-action: 233 Hz
- pole D-action: 2400 Hz
- zero I-action: 80 Hz
- pole I-action: 5 Hz
- bandwidth: 698 Hz
- phase margin: 45°
- maximum sensitivity: 5.7 dB
- sensitivity at rotational frequency (12 Hz): -76 dB

The frequency response of this stable external controller is shown together with that of the internal controller in figure 2.7.

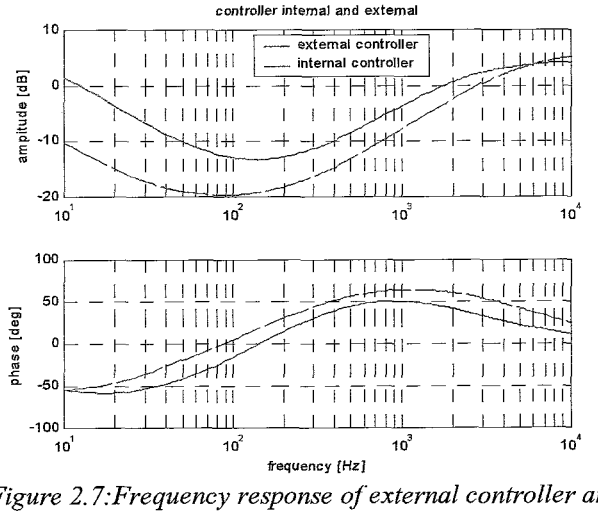

Figure 2.7:Frequency response of external controller and internal controller

The frequency response of the sensitivity (see figure 2.8) is obtained in the same way as in paragraph 2.1.2 except now the internal controller is turned off and the external controller is implemented with dSpace (with a sample frequency of 40 kHz). Again the peaks below 130 Hz have a low coherence and can again be ignored during the fitting of the model.

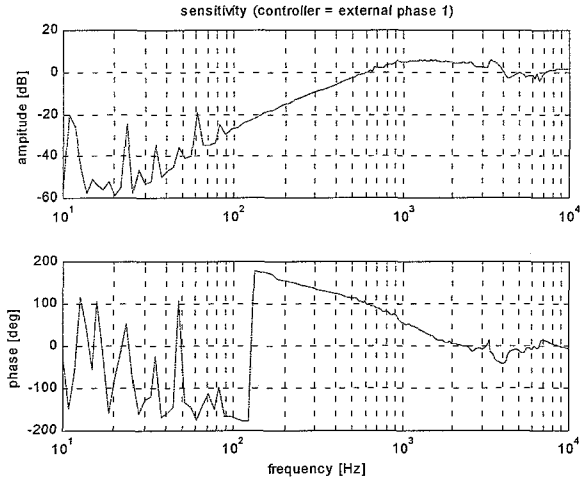

Figure 2.8: Sensitivity (with external controller phase 1)

The open loop is shown in figure 2.9.

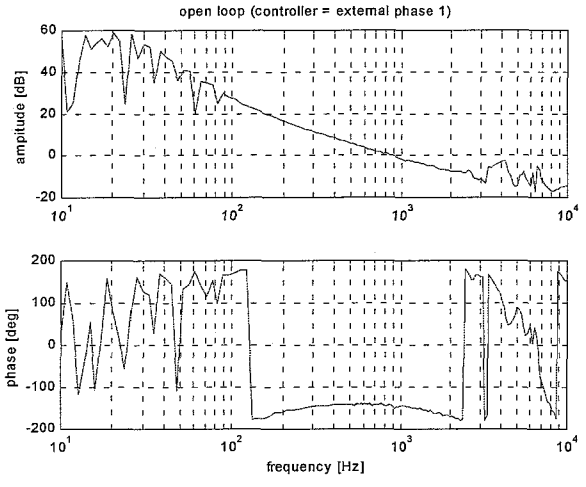

Figure 2.9: Open loop (with external controller (phase 1)

It can be noticed that the bandwidth is not 700 Hz but 900 Hz. The reason is that dSpace causes a delay. So when the controller designed in DIET (C_{diet}) is implemented in dSpace, actually a slightly different controller (C_d=$C_{diet}C_{delay}$), which contains the delay from dSpace, is presented to the plant. A new plant (P_{new}), containing this delay, can be derived from the following equation.

$$S = \frac{1}{1+C_d P} = \frac{1}{1+C_{diet}C_{delay}P} \rightarrow C_{diet}C_{delay}P = S^{-1} - 1 = X \rightarrow P_{new} = \frac{X}{C_{diet}} = C_{delay}P \qquad (2)$$

The frequency response of the plant containing the delay from dSpace together with a 6th order fit is shown in figure 2.10.

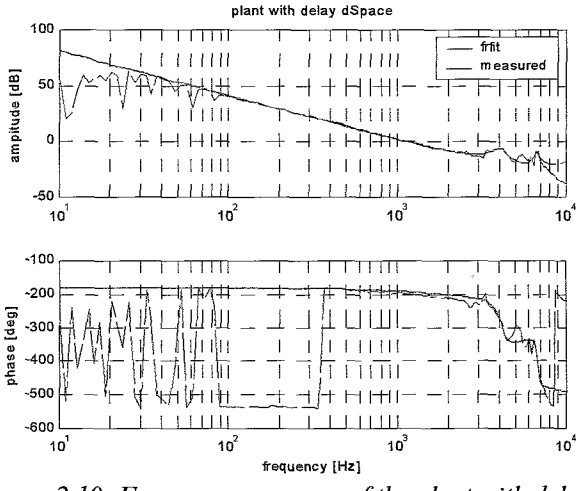

Figure 2.10: Frequency response of the plant with delay dSpace

When the frequency responses of the plant with and without the delay from dSpace are plotted together in one figure, the delay is recognisable (see figure 2.11). The same applies for the 6th order fits (see figure 2.12).

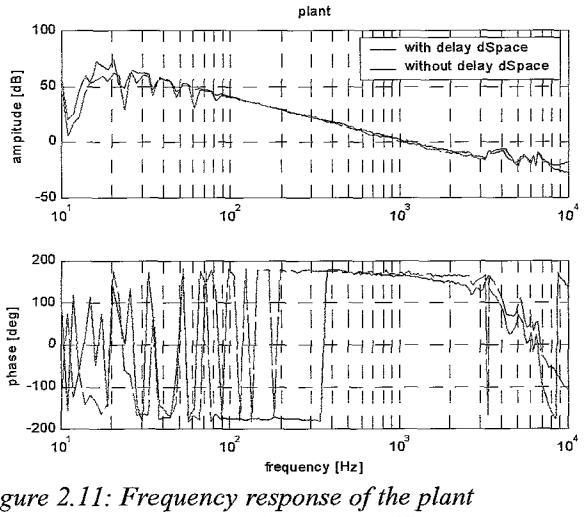

Figure 2.11: Frequency response of the plant with and without delay dSpace

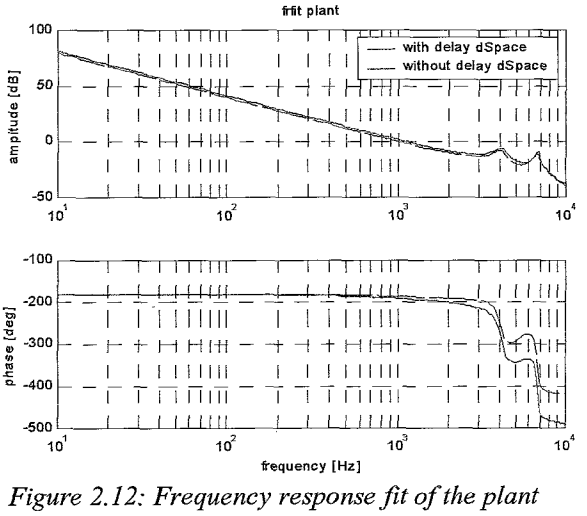

Figure 2.12: Frequency response fit of the plant with and without delay dSpace

The plant containing the delay from dSpace will be used as "the plant" during the rest of this report.

2.3 New external controller (phase 2)

Now the new plant containing the delay of dSpace is known, again an external controller can be designed in DIET using the new plant. The characteristics of this new, also stable, external controller are:

- gain (P-action): 1.7
- zero D-action: 180 Hz
- pole D-action: 2800 Hz
- zero I-action: 80 Hz
- pole I-action: 5 Hz
- bandwidth: 703 Hz
- phase margin: 48°
- maximum sensitivity: 5.0 dB
- sensitivity at rotational frequency (12 Hz): -74.5 dB

The frequency response of this new external controller (phase 2) is shown together with that of the previous external controller (phase 1) and the internal controller in figure 2.13.

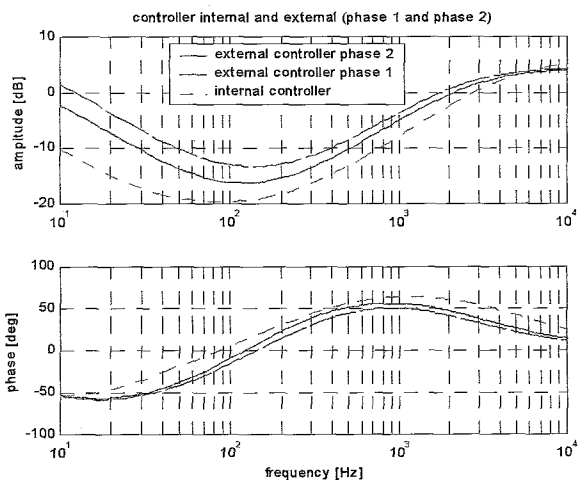

Figure 2.13:Frequency response of external controller (phase 1 and phase 2) and internal controller

4.3 Influence of a phase delay

What would happen when the output of the memory loop is not added to the radial error at exactly the beginning of a period but a little bit earlier or later? In other words what would happen when a phase delay occurs?

To find out what the influence of such phase delay is on the radial error, some other simulations are done each with a different phase delay. The results (maximum radial error versus phase delay) are shown in figure 4.6.

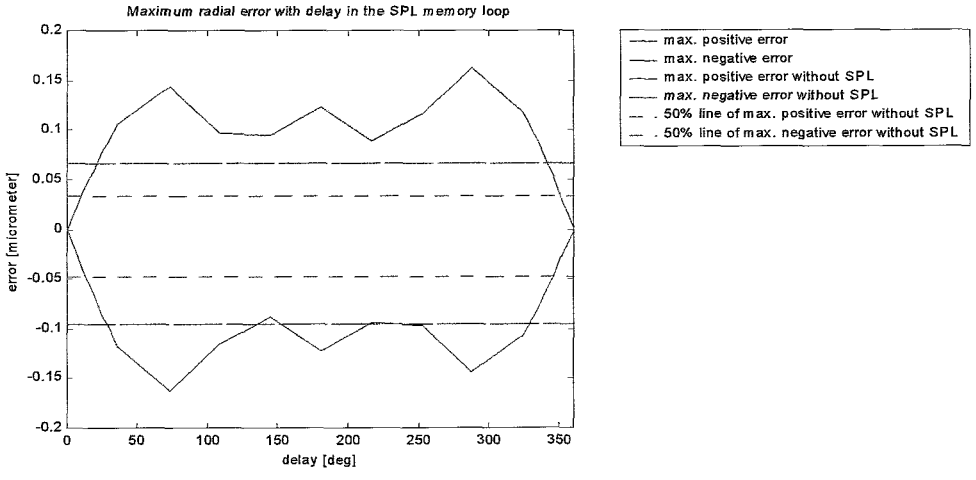

Figure 4.6: The maximum radial error versus phase delay

A delay of 360^0 is equal to a delay of exact 1 period. Every 36^0 a simulation was done and 10 additional simulations where taken between 0 and 36^0 (as well as between 324^0 and 360^0). Figure 4.7 shows a zoom of the regions $0^0 \ldots 36^0$ and $324^0 \ldots 360^0$.

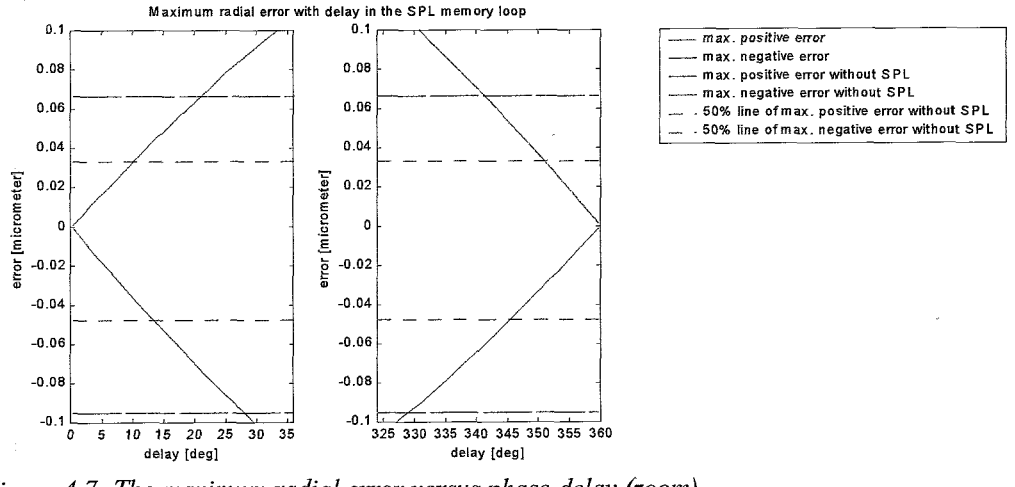

Figure 4.7: The maximum radial error versus phase delay (zoom)

When the phase delay lies between -14.4° ($=345.6^0$) and 13.3^0, an error reduction occurs of at least 50%. The smaller the phase delay, the bigger the error reduction.

The sensitivity, coherence of the sensitivity and the open loop are shown in respectively figure 2.14, figure 2.15 and figure 2.16.

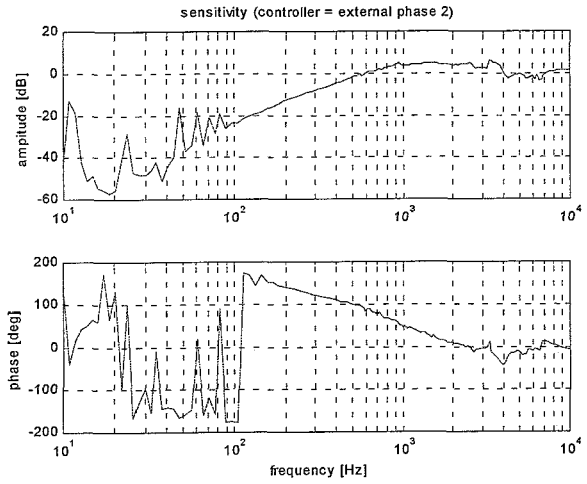

Figure 2.14: Sensitivity (with external controller phase 2)

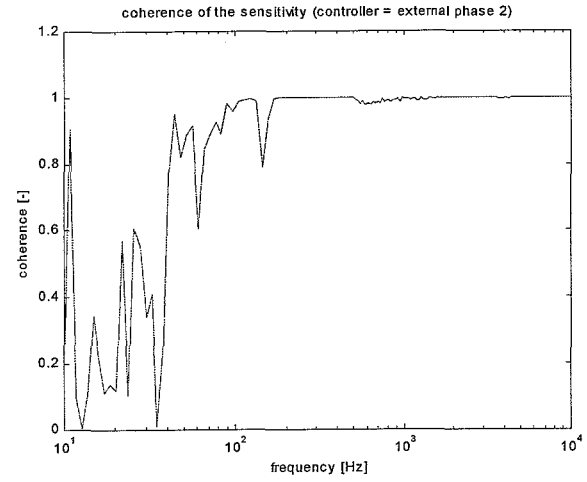

Figure 2.15: Coherence of the sensitivity (with external controller phase 2)

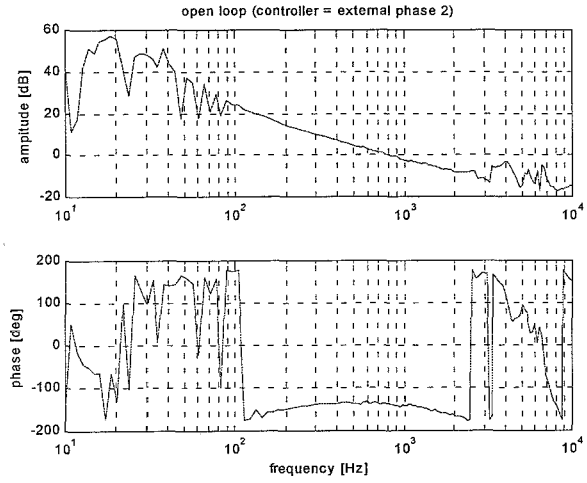

Figure 2.16: Open loop (with external controller phase 2)

During the rest of this report the external controller of phase 2 will be used as "the external controller". The external controller of phase 1 was only temporary needed to derive the plant containing the delay from dSpace.

3 Time domain simulations and experiments

3.1 Simulations

The internal and external PID-controllers, derived in chapter 2, are simulated in Simulink to see how large the radial error would be on simulation level. For the simulation schemes and simulation parameters used in Simulink see appendix B.

To simulate the radial track disturbance a combination of 3 sines is used (presenting the rotational frequency at 12 Hz, and its 2nd and 3rd harmonic (see figure 3.1 and 3.2):

- a sine with a frequency of 12 Hz and an amplitude of 100 μm
- a sine with a frequency of 24 Hz and an amplitude of 25 μm
- a sine with a frequency of 36 Hz and an amplitude of 10 μm

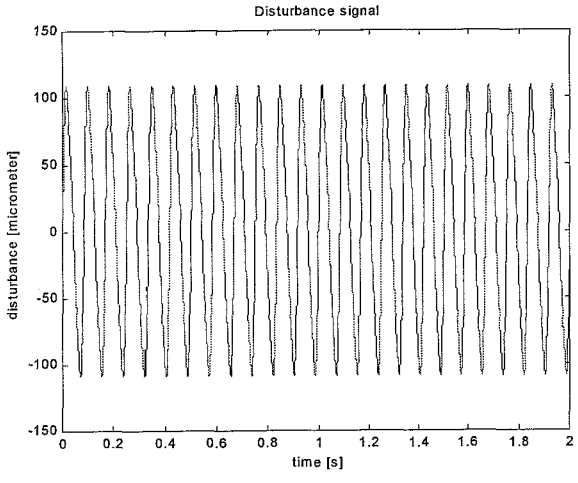

Figure 3.1: Disturbance signal

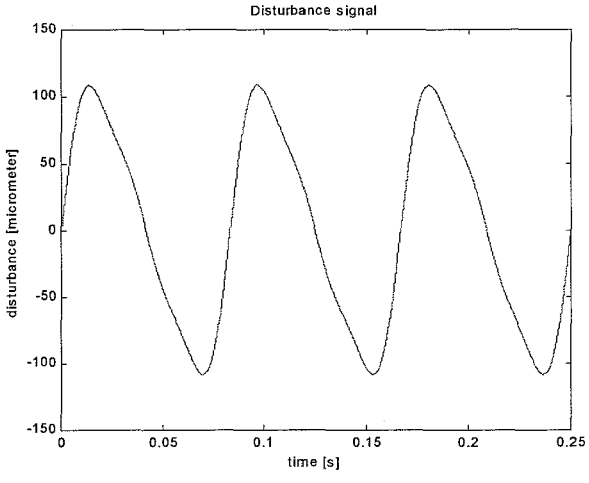

Figure 3.2: Disturbance signal(zoom)

The radial errors that occur using respectively the internal and the external controller, are shown below in figure 3.3 and 3.4.

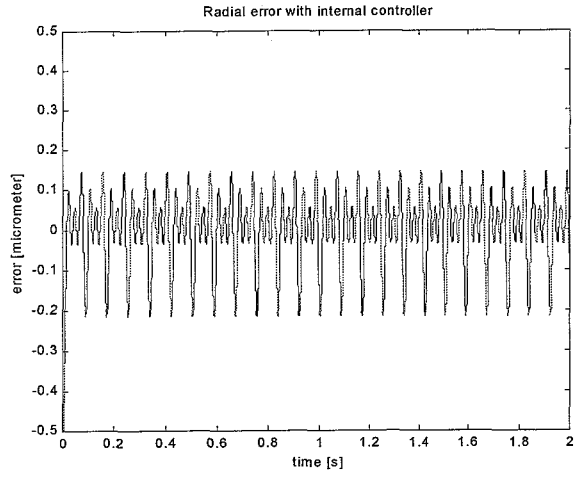

Figure 3.3: Radial error with internal controller

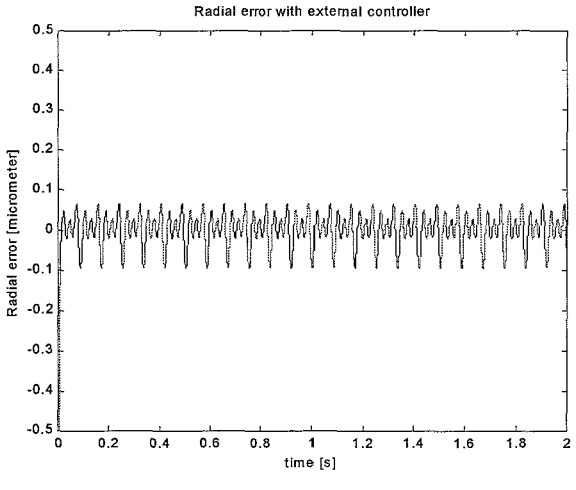

Figure 3.4: Radial error with external controller

The radial errors are periodic signals. When using the internal controller, the error specifications (maximum error < 0.1 μm), stated in chapter 1, are not met. The error lies between +0.1439 and –0.2159 μm. When the external controller is used, these specifications are just met. In that case the error lies between +0.0667 and –0.0954 μm.

3.2 Experiments

The next step is to implement the controllers on the measurement setup to see how big the radial errors are in practice. To get the radial error the signal from AD_rad is measured with Controldesk. There is though a problem. The signal that is measured with Controldesk is in volts, but it can be converted to μm. This is done as follows.

When the radial arm is rapidly moved across the disk, it will come across a lot of tracks. The error signal that then occurs can be approached as a sine. The period of the error signal corresponds to a displacement of the radial arm of 1.6 μm (the displacement between two tracks). So when the error signal is at its maximum the radial arm displaced 0.4 μm. Because the slope of the signal is about 45° when it passes a track, the height of the peaks that occur in the radial error can be assumed to be 0.4 μm as well (see figure 3.5).

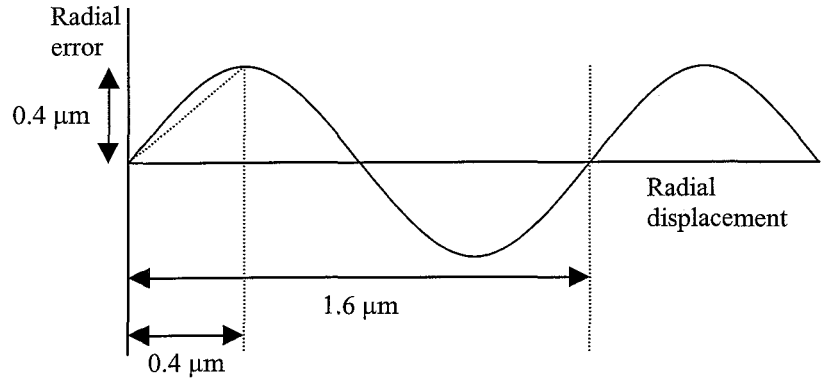

Figure 3.5: Radial error versus radial displacement

So to convert the radial error from volts to μm, first the radial error should be measured when the radial arm is moved rapidly across the disk. The signal shown in figure 3.6 is an example of such measurement.

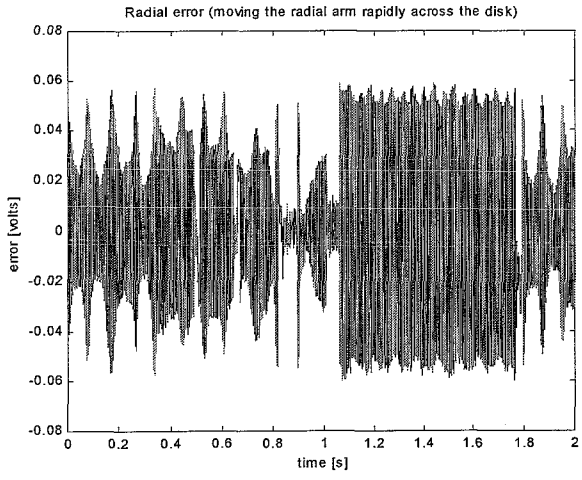

Figure 3.6: Radial error when moving the radial arm rapidly across the disk

The maximum error is +0.0591 and –0.0601 volts. This measurement was repeated several times and the mean maximum error was about 0.06 volts. So 0.06 volts can be compared with 0.4 μm. To translate the radial error from volts to μm, the signals from AD_rad, measured with Controldesk, have to be multiplied by 6.67 (0.4/0.06). The radial errors, obtained with the internal and the external controller, are shown in respectively figure 3.7 and figure 3.8. Also the power spectra of these errors are plotted.

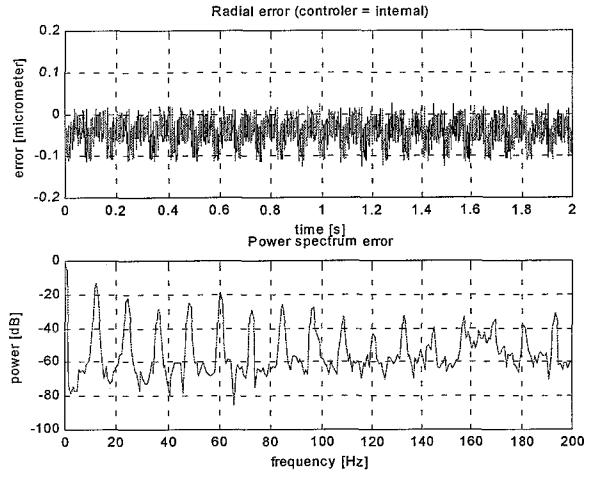

Figure 3.7: Radial error and power spectrum with internal controller

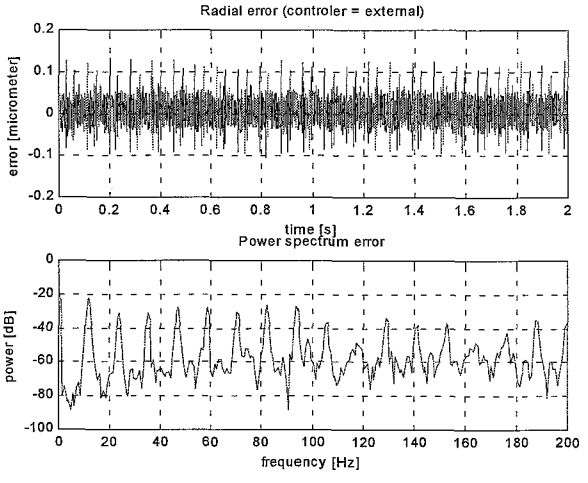

Figure 3.8 Radial error and power spectrum with external controller

The sharp peaks that appear in the error, when using the external controller, are a result of a scratch on the disk and can be neglected.

Both the internal and the external controller have a radial error that lies within the specifications (between +0.01 and –0.11 μm with the internal and between +0.065 and –0.045 μm with the external controller), although it is critical in the case of the internal controller. Why the radial error of the internal controller (critically) meets the specifications during the implementation and during the simulations does not, can be the result of a wrongly chosen disturbance signal in the simulations. Only the rotational frequency and its first 2 harmonics were taken in account. The external controller does meet the specifications in the simulations because its has more gain than the internal controller at low frequencies.

The power spectrum of the errors shows the influence of every disturbance frequency on the error. The rotational frequency and its harmonics have more influence than other frequencies. Also the actual rotational frequency can be simply determined using the power spectrum of the error. For example the 16th harmonic of the rotational frequency, in case of the external controller, lies at 188 Hz. This means that the rotational frequency is 11.75 Hz (188/16).

When the cumulative power spectrum of the error is plotted, the separate contributions of the rotational frequency and its harmonics to the radial error are clearer visible. The cumulative power spectrum of the external error is shown in figure 3.9

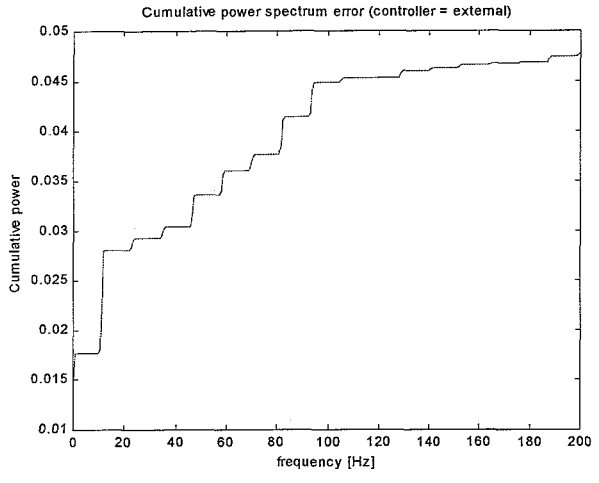

Figure 3.9: Cumulative power spectrum of the radial error with external controller

It is obvious that the rotational frequency has the largest contribution in the error. Second largest are the 4th and the 7th harmonics followed by the 5th and the 8th.

4 Single Period Learning (SPL)

There is been seen that the radial error is a periodic signal. Using this fact can help to reduce the radial error further. Normally this is achieved using repetitive control [2]. However it is interesting to investigate if Single Period Learning (SPL) is useful.

The main idea of SPL is to take 1 period of the radial error, put it into a memory loop and finally add the output signal from the memory loop, as a sort of feedforward signal, to the radial error (without any phase delay). So there is only 1 moment of learning, the moment that 1 period of the radial error is "recorded" in the memory loop.

4.1 Convergence criteria

The convergence criteria for SPL are derived in this paragraph. The block scheme used for this derivation is shown in figure 4.1.

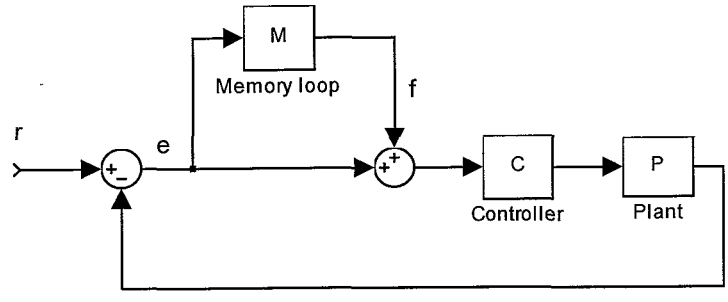

Figure 4.1: Block scheme with SPL memory loop

The following assumptions have been made for the derivation:
- period k is exactly one disk rotation
- e_k = the radial error during rotation k
- f = the output signal from the memory loop
- $r_k = d + n_k$
- r_k = the reference signal (setpoint)
- d = the periodic part (the disturbance) of r_k ($d_{k+1} = d_k$)
- n_k = the non periodic part (measurement noise) of r_k
- assumed that it is allowed to work with transfer functions for these finite time signals

The sensitivity function S is defined as:

$$S = \frac{1}{1 + CP} \tag{3}$$

The complementary sensitivity function T is defined as:

$$T = \frac{CP}{1 + CP} \tag{4}$$

So $S+T=1 \rightarrow S=T-1$ (5)

Using (3), (4) and the block scheme, the following equation can be derived:

$$e=r-CPf-CPe \rightarrow e=\frac{1}{1+CP}r-\frac{CP}{1+CP}f \rightarrow e=Sr-Tf \quad (6)$$

During the first rotation of the disk $f_1 = 0$ so equation (6) becomes:

$$e_1 = Sr_1 - Tf_1 = Sr_1 = S(d+n_1) = Sd + Sn_1 \quad (7)$$

After the first rotation of the disk the learning part of SPL is done and as from the second rotation of the disk, f will be:

$$f = e_1 = Sd + Sn_1 \quad (8)$$

So e_2 will be:

$$e_2 = Sr_2 - Tf = Sr_2 - T(Sd + Sn_1) = Sd + Sn_2 - TSd - TSn_1 \quad (9)$$

Using (5), equation (9) becomes:

$$e_2 = S(1-T)d + Sn_2 - TSn_1 = S^2d + Sn_2 - TSn_1 \quad (10)$$

The final equation that will hold for every disk rotation besides the first, is equation (11):

$$e_k = S^2d + Sn_k - TSn_1 \quad (11)$$

So there can be concluded that the periodic part d of the reference signal will be suppressed with a factor S^2. Of course the disturbance signal will also be amplified around the bandwidth, but at those frequencies the disturbance signal is not much reproducible anymore. The noise however, will be statistically seen raised. The signal n_1 is uncorrelated with n_k, so the variances of these signals will be added to each other.

4.2 Simulation

To see what Single Period Learning is capable of, a simulation is done in Simulink. The same simulation scheme is used as in chapter 3.1, containing the external controller, but it has been extended with the memory loop (see figure 4.2)

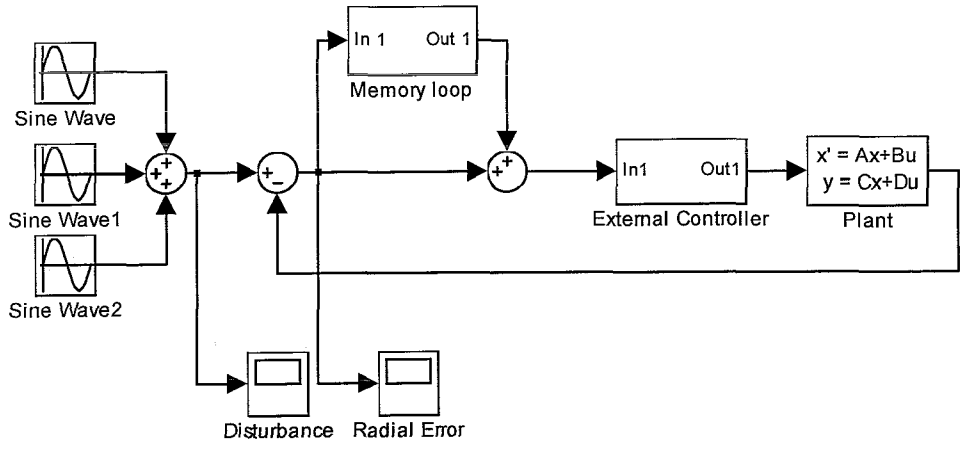

Figure 4.2: Simulink simulation scheme with SPL memory loop

For the disturbance signal, the same signal as in chapter 3.1 is chosen. There is no noise injected in the system.

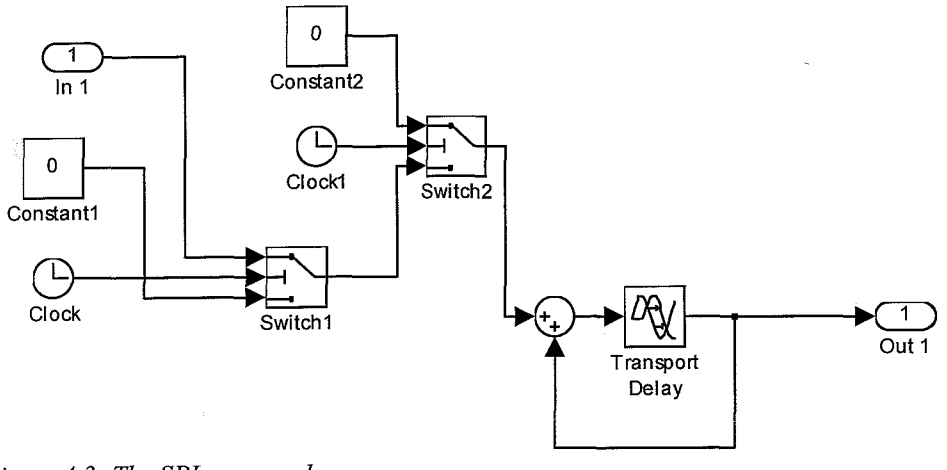

Figure 4.3: The SPL memory loop

The memory loop, shown in figure 4.3, works as follows: the radial error enters the memory loop at "in 1". The 2 "switches" make sure that the signal that arrives at the "transport delay" contains only 1 period of the radial error. The "transport delay" causes a delay of exact 1 period and keeps repeating its own output (due to the feedback loop).

The period of the radial error that is repeated in the memory loop has a length of $1/f_m$ seconds. F_m is the frequency used in the memory loop and has to be taken equal to the rotational frequency f_{rot} (= 12 Hz.).

To be sure that the transient response, caused by the activation of the simulation, is gone, the memory loop is activated by "switch1" after 0.16 seconds ($2/f_m$). The 3rd period of the radial error was captured in the memory loop and exactly at the beginning of the 4th period the output signal from the memory loop was added to the radial error. So no phase delay occurred. The radial error that is measured during this simulation is shown in figure 4.4 and a zoom in figure 4.5.

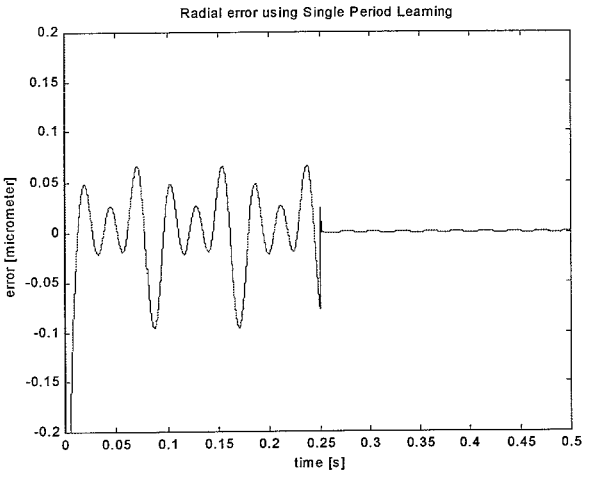

Figure 4.4: Radial error using SPL

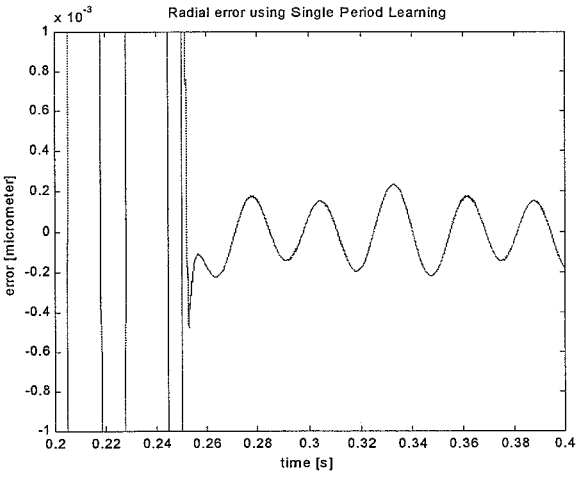

Figure 4.5: Radial error using SPL (zoom)

Using Single Period Learning causes a tremendous decrease of the radial error, which lies now between the +0.23 nm and –0.22 nm. That implies a maximum error reduction of a factor 434.

4.4 Influence of noise

To see what influence noise has on the performance of SPL, two simulations were done. The noise used in these two simulations is white noise, has a sample frequency of 250 Hz, a power of $1e^{-7}$ and is injected as measurement noise in the feedback loop. The noise is plotted in figure 4.8. There is no phase delay during these simulations. The resulting radial error is shown in figure 4.9.

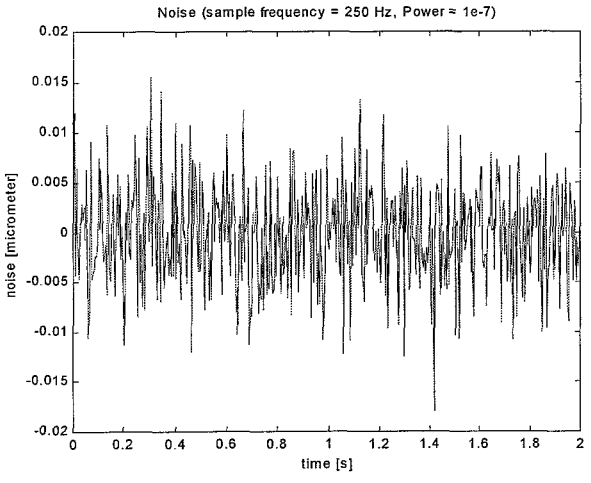

Figure 4.8: Noise signal

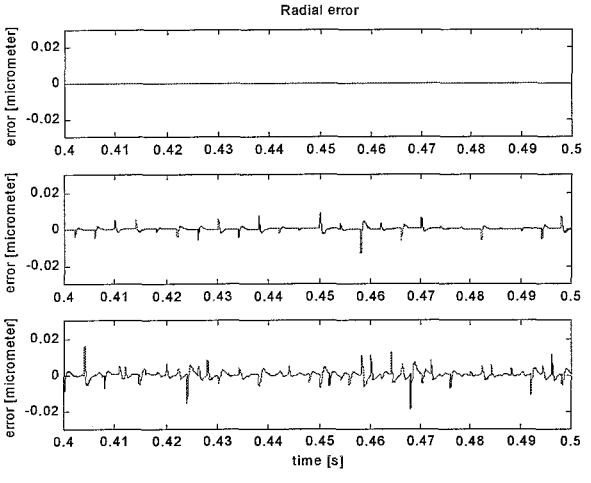

Figure 4.8: Radial error; 1st figure: no noise injected; 2nd figure: noise injected after learning process (no noise in memory loop); 3rd figure: noise injected at beginning of simulation (also noise in memory loop)

In the first figure the radial error is plotted without injecting the noise. In the second figure the noise is injected after the learning process in the memory loop took place. So the output signal of the memory loop contained no noise. The noise is simply added to the radial error. In the third figure the noise is injected at the beginning of the simulation so the noise is also put in the memory loop. Because the output signal of the memory loop contained noise, the noise part in the radial error is amplified.

To see how large this noise amplification is, another simulation is done without the disturbance signal. So the radial error would only contain the influence of the noise. The resulting radial error is shown in figure 4.10 (The output signal of the memory loop is added to the radial error at the time of 0.25 seconds).

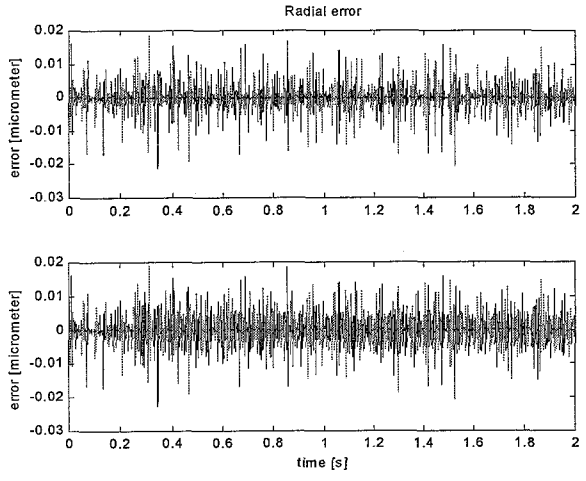

Figure 4.10: Radial error without using disturbance signal; 1st figure: noise injected after learning process (no noise in memory loop); 2nd figure: noise injected at beginning of simulation (also noise in memory loop)

The noise amplification can be clearly seen. Using the 2nd norm of the signals the following equation is obtained (see appendix C for validation):

$$\|e_l\|_2 = \sqrt{\|f_n\|_2^2 + \|e_{nl}\|_2^2} \tag{12}$$

with: e_l = the radial error signal when the noise is learned in the memory loop
e_{nl} = the radial error signal when the noise is not learned in the memory loop
f_n = the output signal from the memory loop containing the noise

Theoretically $\|f_n\|_2$ and $\|e_{nl}\|_2$ should be the same and uncorrelated. In the simulations no exact white noise can be simulated so there is a little correlation between the two signals. In theory $\|e_l\|_2$ should be an addition of two uncorrelated noise sequences, so equation (12) becomes:

$$\|e_l\|_2 = \sqrt{\|f_n\|_2^2 + \|e_{nl}\|_2^2} = \sqrt{2 \cdot \|e_{nl}\|_2^2} = \sqrt{2} \cdot \|e_{nl}\|_2 \tag{13}$$

So due to the memory loop the measurement noise will be amplified with a factor $\sqrt{2}$.

4.5 Influence of not knowing the rotational frequency exactly

During the simulations that have been done in this chapter the rotational frequency (f_{rot}) was exactly known. So it was easy to obtain exactly one period of the radial error to put in the memory loop. The period that was taken had a length of $1/f_m$ seconds and f_m (the frequency used in the memory loop) was chosen the same as f_{rot} = 12 Hz. But what would happen if the rotational frequency is not exactly known and f_m therefore is not taken equally to f_{rot}? In that case not exactly one period of the radial error will be taken in the memory loop, but a signal that is a little bit larger or smaller than one period. The radial error that occurs when f_{rot} = 12 Hz and f_m = 11 Hz is shown in figure 4.11 (there is no phase delay and no noise).

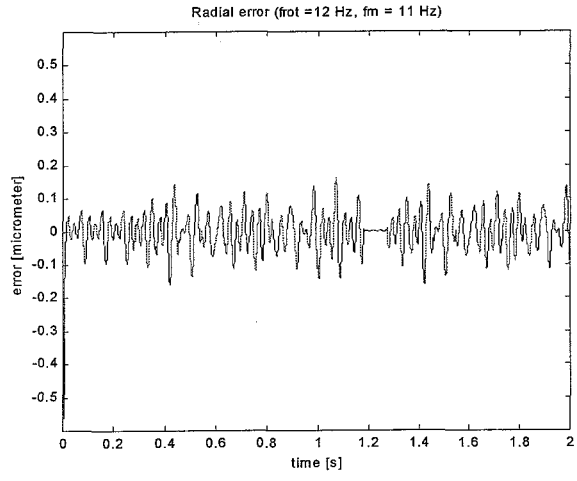

Figure 4.11: Radial error; f_{rot} = 12 Hz and f_m = 11 Hz

The radial error (+/- 0.1612 μm) is even larger than when SPL is not used. So it is obviously necessary to know the rotational frequency exactly to use SPL properly. At one point in figure 4.11 (after about 1.2 seconds) the radial error is extremely small again for a short time. This is the point where the period of the output signal of the memory loop and the period of the radial error start exactly at the same time. For a time-period, which is equal to the smallest period of the two signals, the signals overlap each other resulting in the same radial error as discussed in chapter 4.2. At what time these overlap points (OP) occur, can be calculated with the following equation:

$$OP = T_b + k \cdot T_o = \frac{2}{f_m} + k \cdot \frac{\frac{1}{f_{rot} f_m}}{\left| \frac{1}{f_{rot}} - \frac{1}{f_m} \right|} = \frac{2}{f_m} + k \cdot \frac{1}{|f_m - f_{rot}|} \qquad (14)$$

k=1,2,3,...

T_o = is the period between two overlap points
T_b = the time that SPL is not operational in the beginning of a simulation to be sure the transient response is gone and is not taken into the memory loop.

When f_m is taken closer to f_{rot}, the maximum amplitude of the radial error is not getting any smaller (+/- 0.1622 μm). Only the time between two overlap points is getting longer. In figure 4.12 and 4.13 the radial errors are shown with f_{rot} = 12 Hz and respectively f_m = 11.9 Hz and f_m = 11.95 Hz

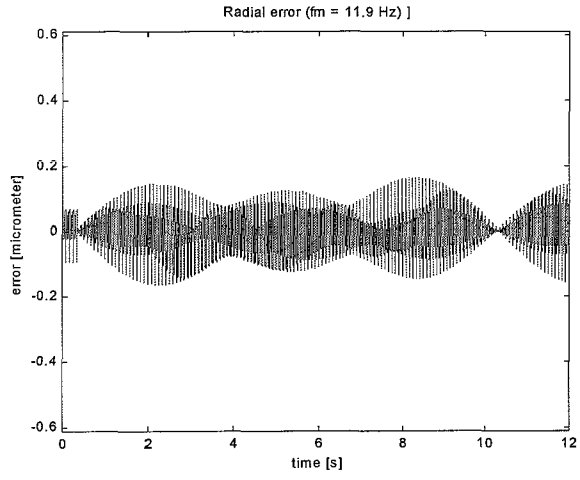

Figure 4.12: Radial error; f_{rot} = 12 Hz and f_m = 11.9 Hz

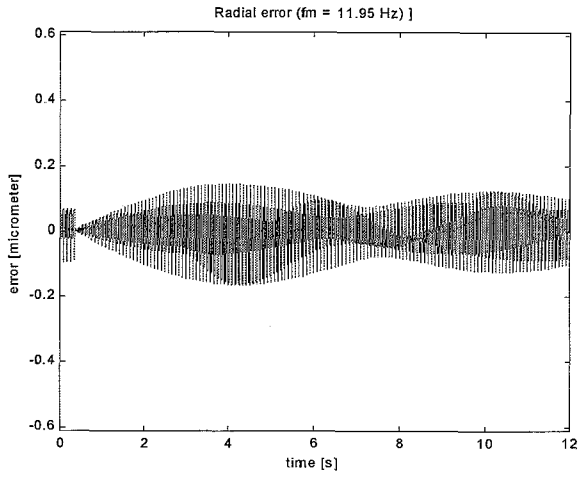

Figure 4.13: Radial error; f_{rot} = 12 Hz and f_m = 11.95 Hz

When f_m = 11.9 Hz: OP = 0.17 + k*10 = 10.17, 20.17, etc.
When f_m = 11.95 Hz: OP = 0.17 + k*20 = 20.17, 40.17, etc.

Because the output signal from the memory loop has a different period than the radial error, it can be seen as a signal with the same period length as the radial error and containing a time dependent phase delay. Each period the output signal from the memory loop corresponds with a signal with a different phase delay. The delay of period k (D_k), in degrees, can be obtained using the following equation:

$$D_k = k \cdot \left(\frac{1}{f_m} - \frac{1}{f_{rot}} \right) \cdot f_{rot} \cdot 360^0 = k \cdot \left(\frac{f_{rot}}{f_m} - 1 \right) \cdot 360^0 \qquad (15)$$

A delay of 360^0 is equal to a delay of 1 period of the radial error ($1/f_{rot}$).

When f_m = 11.9 Hz: $D_k = k*3.02^0$.
When f_m = 11.95 Hz: $D_k = k*1.51^0$.

So when f_m is chosen closer to f_{rot}, the delay difference between two successive periods will be smaller. The radial error is not getting bigger than 0.1622 μm because that is also the maximum radial error when a delay occurs (see figure 4.6 in chapter 4.3). There is a great resemblance between figure 4.12 and figure 4.6, which confirms the theory described here.

4.6 Robust control

In an attempt to make SPL robust for not knowing the rotational frequency exactly, a method presented by Steinbuch [3], which performs well in case of repetitive control, was used. The main idea of this technique is to take 3 successive periods (e_1, e_2 and e_3: each with a length of $1/f_m$) of the radial error into the memory loop instead of one and multiply these periods with weight factors (respectively 3, -3 and 1). The memory loop that was used is shown in appendix D. So the output signal from the memory loop will be a repetition of the signal: $3e_1-3e_2+e_3$.

For the simulation f_{rot} = 12 Hz and f_m = 11.9 Hz was used. The radial error is shown in figure 4.14 without the robust control and in figure 4.15 with robust control.

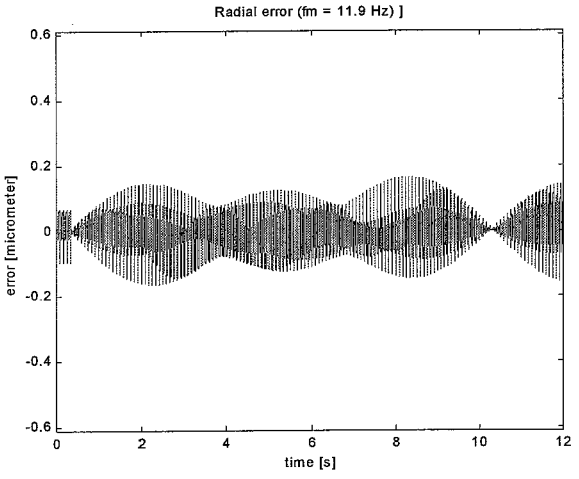

Figure 4.12: Radial error; f_{rot} = 12 Hz and f_m = 11.9 Hz without robust control

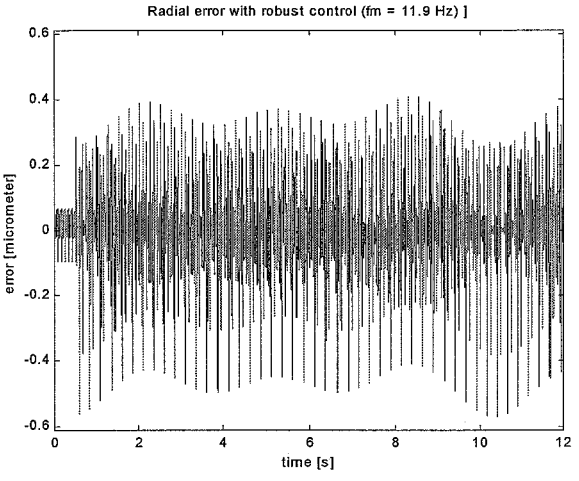

Figure 4.13: Radial error; f_{rot} = 12 Hz and f_m = 11.9 Hz with robust control

Unfortunately the robust control used in the case of repetitive control does not work well at all using SPL.

4.7 Analysis

In case that the correct frequency info is not available, the following problem occurs:

$$\min_{\omega_i}\left(\sin(2\pi f_0 t)-\sum_{i=1}^{n}\omega_i \sin(2\pi f_i t)\right) \qquad (16)$$

with f_0 the given frequency of the disturbance and $f_i \neq f_0$.

To solve this problem is for further study.

5 Conclusions and recommendations

The main goal of this report was to keep the radial error as small as possible and at least 0.1 μm. In order to achieve this an external PID-controller was designed and tested. With this PID-controller the error specification of 0.1 μm was met. To obtain a smaller radial error Single Period Learning (SPL) was introduced.

The conclusions about SPL that can be drawn are:

- SPL decreases the radial error spectacular. The radial error is +/- 0.22 nm when no phase delay occurs, no noise is injected and the rotational frequency is exactly known.
- When the phase delay lies between -14.4^{o} ($=345.6^{0}$) and 13.3^{0}, the error reduction will be at least 50%. The smaller the phase delay is that occurs the bigger the radial error reduction will be.
- SPL amplifies noise with a factor $\sqrt{2}$.
- SPL is very sensitive for not knowing the rotational frequency exactly.
- The robust control technique used for repetitive control does not work well with SPL.

Recommendations:

- Try to implement SPL on an experimental setup to see if the results gained in the simulations also apply in practice
- Develop a filter that filters out the noise before learning.
- Try to develop a robust control technique for SPL to make it less sensitive for not knowing the rotational frequency exactly.

Bibliography

[1] J. Janssens, "Characterisation of optical discs", DCT 2001-14, Eindhoven university of technology

[2] T. d. Hoog, "Stability and performance of memory loop filtered control systems", *PATO Cursus Repetitive and Learning Control*, Delft university of technology

[3] M. Steinbuch, "Repetitive control for systems with uncertain period-time, with application to a compact disc drive", *Proc. 1st IFAC conference on Mechatronic Systems*, 18-20 September 2000, Darmstadt, pp.409-414.

[3] M.J. v.d. Molengraft, "Disturbance cancellation in Compact Disk Applications", DCT 2001-61, Eindhoven university of technology

Appendix A: Settings Virtual Swept Sine (VSS)

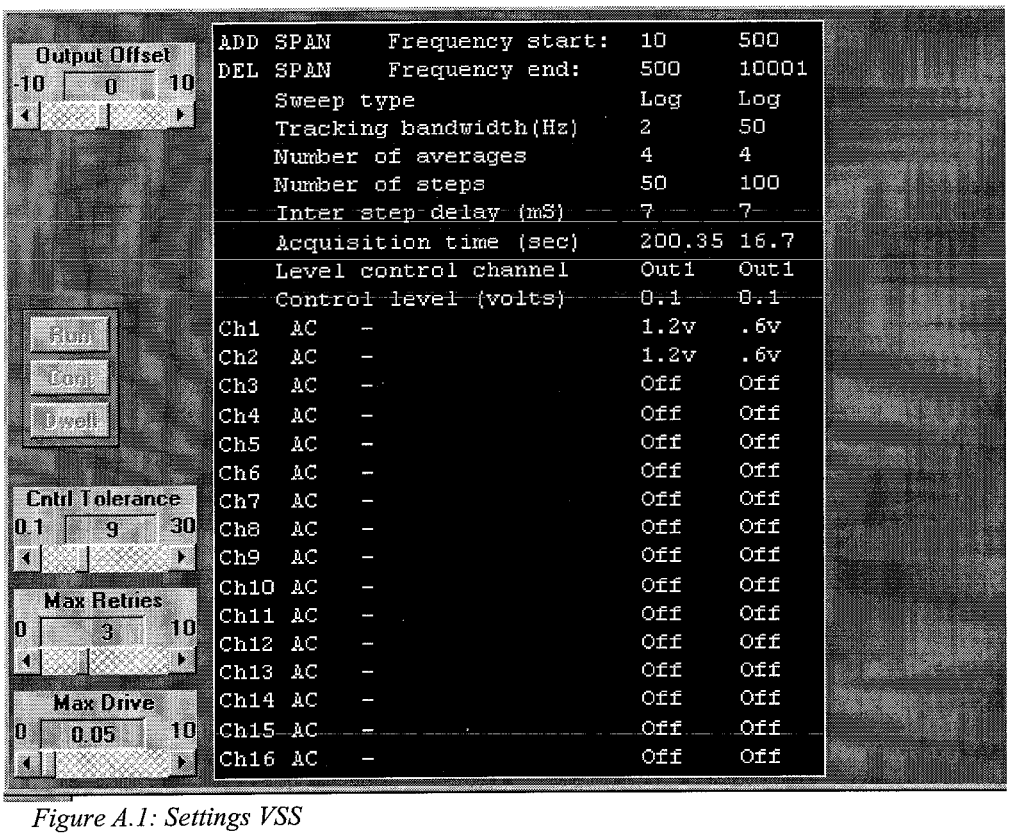

ADD SPAN		Frequency start:	10	500
DEL SPAN		Frequency end:	500	10001
	Sweep type		Log	Log
	Tracking bandwidth(Hz)		2	50
	Number of averages		4	4
	Number of steps		50	100
	Inter step delay (mS)		7	7
	Acquisition time (sec)		200.35	16.7
	Level control channel		Out1	Out1
	Control level (volts)		0.1	0.1
Ch1	AC	-	1.2v	.6v
Ch2	AC	-	1.2v	.6v
Ch3	AC	-	Off	Off
Ch4	AC	-	Off	Off
Ch5	AC	-	Off	Off
Ch6	AC	-	Off	Off
Ch7	AC	-	Off	Off
Ch8	AC	-	Off	Off
Ch9	AC	-	Off	Off
Ch10	AC	-	Off	Off
Ch11	AC	-	Off	Off
Ch12	AC	-	Off	Off
Ch13	AC	-	Off	Off
Ch14	AC	-	Off	Off
Ch15	AC	-	Off	Off
Ch16	AC	-	Off	Off

Figure A.1: Settings VSS

Appendix B: Simulink simulation schemes and parameters

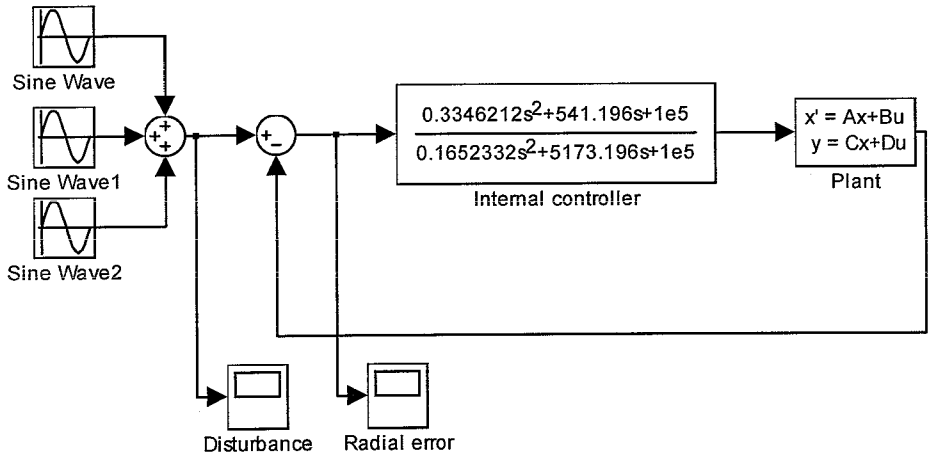

Figure B.1: Simulink simulation scheme with internal controller

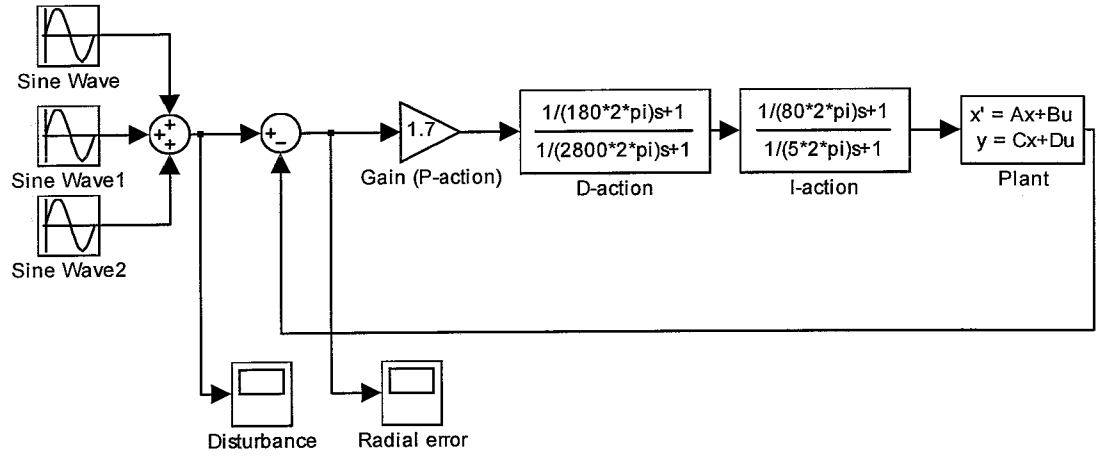

Figure B.2: Simulink simulation scheme with external controller

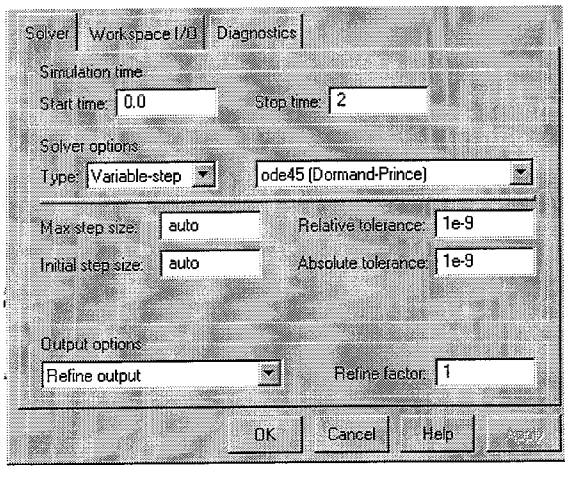

Figure B.3: Simulation parameters

Appendix C: Simulation results for influence noise

Every simulation another realisation of the noise (seeds) is used.

Simulation	$\|e_{nl}\|_2$	$\|f_n\|_2$	$\|e_l\|_2$	$\sqrt{\|f_n\|_2^2 + \|e_l\|_2^2}$	$\frac{\sqrt{\|f_n\|_2^2 + \|e_l\|_2^2}}{\|e_l\|_2}$
1	0.3598	0.3440	0.5011	0.4978	0.9934 %
2	0.3884	0.4259	0.5807	0.5764	0.9926 %
3	0.3720	0.3390	0.5069	0.5033	0.9929 %
4	0.3977	0.3131	0.5164	0.5061	0.9801 %
5	0.3753	0.2185	0.4408	0.4343	0.9854 %
6	0.3757	0.3115	0.4955	0.4880	0.9851 %
7	0.3981	0.2791	0.4918	0.4862	0.9886 %
8	0.3374	0.3229	0.4711	0.4670	0.9914 %
9	0.4147	0.3835	0.5615	0.5649	1.0059 %
10	0.3686	0.2235	0.4377	0.4311	0.9850 %

Tabel C.1: Simulation results for influence noise

Appendix D: Memory loop used for robust control

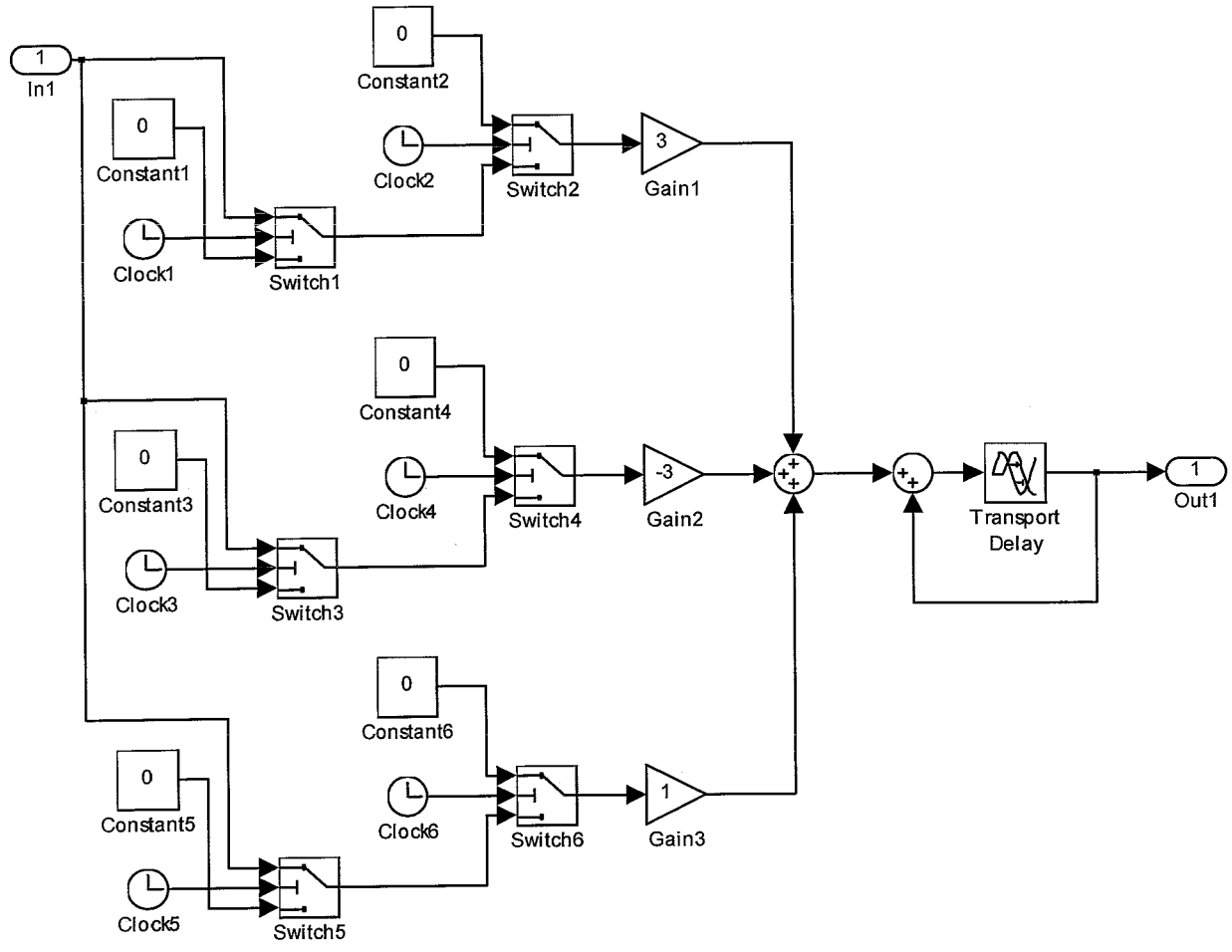

Figure D.1: Memory loop used for robust control